JOURNAL OF SPACECRAFT AND ROCKETS
Vol. 57, No. 1, January–February 2020

Arcjet Thruster Influence on Local Magnetic Field Measurements from a Geostationary Satellite

S. Califf* and T. M. Loto'aniu*
Cooperative Institute for Research in Environmental Sciences, Boulder, Colorado 80305
D. Early†
Chesapeake Aerospace, Manteo, North Carolina 27954
and
M. Grotenhuis‡
Science Systems and Applications, Inc., Lanham, Maryland 20706

https://doi.org/10.2514/1.A34546

The 16th Geostationary Operational Environmental Satellite (GOES-16) is the first satellite launched from National Oceanic and Atmospheric Administration's (NOAA's) next-generation Geostationary Operational Environmental Satellite-R series. Observations from GOES-16 are used by the NOAA to provide terrestrial and space weather forecasts, warnings, and alerts. The magnetometer (referred to as MAG) on GOES-16, which monitors the geomagnetic field, consists of two triaxial fluxgate magnetometers mounted on an 8.5 m boom. The spacecraft uses hydrazine arcjet thrusters for station keeping; when the arcjets are fired, a large magnetic field disturbance contaminates the MAG data. Here, the characteristics of the arcjet contamination are described and possible physical mechanisms for the magnetic field disturbance are discussed. The arcjets operate for ∼90 min approximately every four days, and the contamination significantly impacts the utility of the MAG data for space weather operations. The arcjets create step changes in the geomagnetic field observations of up to about 20 nT (∼20% of the nominal field strength). Two separate physical mechanisms are suggested: a large-scale diamagnetic effect caused by the dense plasma in the thruster plume, and a local current source caused by plasma pressure gradients near the thruster.

Nomenclature

B	=	magnetic field, nT
J	=	current density, $A \cdot m^{-2}$
k	=	Boltzmann's constant, $m^2 \cdot kg \cdot s^{-2} \cdot K^{-1}$
m	=	mass, kg
n	=	number density, m^{-3}
P	=	pressure, Pa
q	=	elementary charge, C
r_{gyro}	=	particle gyroradius about the magnetic field, m
T	=	temperature, K
V	=	flow speed, $m \cdot s^{-1}$
μ_0	=	permeability of free space, $H \cdot m^{-1}$
$v_\perp$	=	particle speed perpendicular to the magnetic field, $m \cdot s^{-1}$
ρ	=	mass density, $kg \cdot m^{-3}$

Subscripts

EPN	=	Earthward-poleward-normal coordinate system
SC	=	spacecraft
XYZ	=	spacecraft-fixed coordinate system

Received 13 May 2019; revision received 13 September 2019; accepted for publication 21 September 2019; published online Open Access 26 November 2019.

*National Oceanic and Atmospheric Administration–National Centers for Environmental Information; also Research Scientist, University of Colorado Cooperative Institute for Research in Environmental Sciences/National Oceanic and Atmospheric Administration–National Centers for Environmental Information.

†Mission Systems Engineer, Geostationary Operational Environmental Satellite-R Flight Project, NASA Goddard Space Flight Center.

‡GOES-R Magnetometer Instrument Systems Engineer, Geostationary Operational Environmental Satellite-R Flight Project, NASA Goddard Space Flight Center.

I. Introduction

SPACECRAFT are increasingly using electric propulsion systems for station-keeping and orbital maneuvers due to the improved efficiency relative to traditional thrusters. Arcjet thrusters are a type of electric propulsion that adds additional energy to the exhaust, resulting in increased thrust by applying a current to the propellant before it exits the nozzle. The 16th Geostationary Operational Environmental Satellite (GOES-16) uses 2 kW hydrazine arcjet thrusters for station-keeping maneuvers, achieving a specific impulse I_{sp} of ∼600 s [1]. Part of the exhausted gas is ionized, and this plasma in the thruster plume interacts with the local space environment. Previous studies of the on-orbit characteristics of arcjet thrusters and other electric propulsion plasma plumes are limited: particularly regarding the effects on the local magnetic field. This study addresses arcjet thruster impacts on measurements from the scientific magnetometers on board GOES-16.

Grebnev et al. [2] observed electromagnetic fluctuations in the 5–20 kHz and 0.8–1.2 MHz frequency ranges related to xenon plasma thruster operations on the Meteor satellites in the ionosphere. The authors noted that the plasma jet had greater interaction with the ambient geomagnetic field when fired perpendicular to the magnetic field. The dependence of plasma plume dynamics on the relative orientation to the geomagnetic field was also discussed by Gabdullin et al. [3] using density measurements of a xenon arcjet on the International Space Station, but it was noted that the currents associated with the plasma plume had little effect on the ambient magnetic field.

In low Earth orbit (LEO), the geomagnetic field is on the order of 30,000 nT, and at geostationary orbit (GEO), the geomagnetic field is typically ∼100 nT; so, the relative effect of the plasma plume on the ambient magnetic field is expected to be much larger at GEO than at LEO. The Express-A geosynchronous communication satellites were equipped with xenon hall thrusters for station keeping, and the plasma density, temperature, and electric field were measured using onboard sensors [4]. The on-orbit plasma measurements did not agree with ground tests, and the differences were attributed to collisional dynamics in the laboratory environment that were not present on orbit.

In terms of magnetic field observations near GEO or geostationary transfer orbit, contamination of magnetic field measurements was

observed on the Combined Release and Radiation Effects Satellite (CRRES) spacecraft during chemical release experiments. Canisters of barium on board CRRES were exploded at various altitudes in the ionosphere and magnetosphere, and diamagnetic cavities due to the dense plasma cloud were formed that effectively canceled the ambient magnetic field with scale sizes up to 30 km [5]. Although there are similarities between the CRRES diamagnetic cavities and the magnetic field effects related to the arcjets observed on GOES-16, the CRRES experiments involved a sudden introduction of ∼10 kg of barium into the ambient environment, whereas the GOES-16 arcjets gradually released only a fraction of a kilogram of propellant over 90 min.

This study, to our knowledge, is the first to show onboard observations of dc magnetic contamination caused by arcjet thrusters. The arcjet firing results in a partial cancelation of the ambient magnetic field. In Sec. II, an example of the typical arcjet contamination observed in the magnetometer (MAG) data is presented and the signature characteristics are described. Section III shows the results of statistical analysis of the arcjet contamination events, and the correlation between the arcjet disturbance magnitude and the strength of the ambient magnetic field is presented in Sec. IV. Possible physical mechanisms for generating the contamination magnetic fields are discussed in Sec. V, and Sec. VI concludes with a summary of the results.

II. GOES-16 Magnetometers and Arcjet Thruster Locations

A. GOES-16 Magnetometers

GOES-16 magnetic field observations are a continuation of over 40 years of Geostationary Operational Environmental Satellite (GOES) magnetometers monitoring Earth's magnetic field at GEO. These measurements are used in the National Oceanic and Atmospheric Administration's (NOAA's) Space Weather Prediction Center for detecting space weather events such as geomagnetic storms, substorms, and magnetopause crossings inside of GEO. The MAG data are also used to calculate pitch angles for in situ energetic particle measurements on GOES-16, as well as to validate new global space weather models. Additionally, GOES magnetometer data are some of the most used datasets in the space physics research community, and the GOES measurements have been an important input for developing empirical magnetospheric magnetic field models [6]. The geostationary location is ideal for measuring the effect of several magnetospheric current systems [7], and the data play an important role in advancing our understanding of the response of the magnetosphere and the coupled Earth system to solar activity.

The latest iteration of the GOES magnetometers are the GOES-R series magnetometers, and the GOES-16 MAG is the first in the series. The GOES-16 MAG performance characteristics are similar to previous GOES magnetometers, with the main advancement of a 10 Hz sample rate with a 2.5 Hz antialiasing filter [8]. Previous GOES magnetometers had a 2 Hz sample rate and a 0.5 Hz antialiasing filter. The MAG consists of two three-axis vector fluxgate magnetometers mounted on a long boom to reduce the effect of magnetic fields originating from the spacecraft. The inboard sensor is located 6.3 m from the spacecraft, and the outboard sensor is located 8.5 m from the spacecraft at the end of boom.

B. Arcjet Thruster Locations Relative to the Magnetometers

GOES-16 uses arcjet thrusters for periodic station-keeping maneuvers to maintain the desired location in geostationary orbit. A schematic of the GOES-16 spacecraft with the arcjet thrusters and MAG boom is shown in Fig. 1. There are four arcjet thrusters on GOES-16 numbered 13, 14, 15, and 16; and they are fired in pairs of either the 13/15 thrusters or the 14/16 thrusters for approximately 90 min every four days. The thruster nozzles point in the $-Y$ direction expressed in the body-fixed spacecraft frame called the attitude control reference frame (ACRF). In the nominal pointing mode, the $+Z$ axis points toward the center of the Earth, and $+Y$ is aligned with the orbit normal vector. The nominal relationship between spacecraft coordinates and Earthward-poleward-normal (EPN) coordinates is also shown. The geomagnetic field is generally aligned in the poleward direction, which is also aligned with the thrusters along the spacecraft $-Y$ axis.

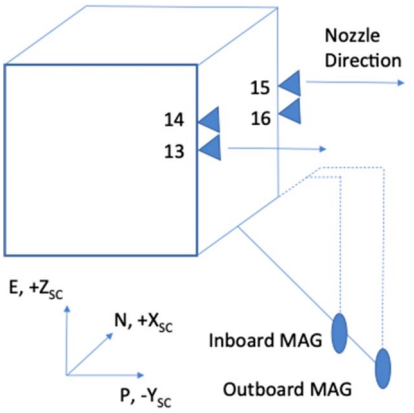

Fig. 1 Spacecraft diagram showing relative locations and orientations of the arcjet thrusters and the magnetometers.

III. Arcjet Signatures in the Magnetic Field Measurements

The effect of the arcjets on GOES-16 magnetometer measurements is shown in red in Fig. 2. The arcjets fired from 18:10 to 19:40 Universal Time (UT), creating a steplike decrease in the magnetic field mostly in the P (poleward) component (Fig. 2b), which is approximately aligned with the geomagnetic field. In this example, a coronal mass ejection impacted Earth's magnetosphere at 15:30 UT, creating the initial increase in the P component of the magnetic field [9]; shortly after the arcjets turned off, a second shock from the solar wind impacted the magnetosphere, causing additional fluctuations in the magnetic field. The arcjet disturbance poses a problem for using the GOES-16 MAG in space weather operations because the magnitude of the offset is similar in magnitude to real geomagnetic activity. With the arcjets firing for ∼90 min every four days, the magnetic contamination creates significant data gaps for an instrument that is required to provide continuous data for operations. This is a motivation to understand and correct for the arcjet effect measured by the magnetometer.

Data from the nearby 13th Geostationary Operational Environmental Satellite (GOES-13) magnetometer are also shown in Fig. 2 as a general indication of the unperturbed geomagnetic field. The spacecraft were separated by 1 h in local time, with GOES-16 located at 90° W longitude and GOES-13 stationed at 75° W longitude. When comparing the GOES-16 magnetic field observations within the arcjet firing period to the GOES-13 measurements, geophysical variations are qualitatively preserved. This indicates that the arcjet offset is reasonably stable during the firing period and provides some confidence that the true magnetic field can be recovered using a correction algorithm. The magnetic field time series observed by GOES-13 and GOES-16 are not expected to be in exact agreement due to the spatial separation between the spacecraft, and there are known calibration differences between the two instruments. Also, the GOES-16 10 Hz magnetic field observations show more detailed features than in the 2 Hz GOES-13 magnetic field data.

Figure 3 shows an example of the initial transient as the arcjets are turned on. There is a gradual change in the magnetic field as currents to the thrusters are ramped up over several minutes, and there are steps in the magnetic field that are directly correlated with changes in the thruster currents. Some of the step responses are followed by a slower settling period that is difficult to distinguish between possible real changes in the geomagnetic field over these timescales.

At the end of the arcjet burn, the currents are turned off quickly and there is a rapid change in the magnetic field. Figure 4 shows the measured magnetic field from the inboard (IB) and outboard (OB) magnetometers as the arcjets are turned off. There are four arcjet thrusters on the spacecraft, and each arcjet event uses two of the

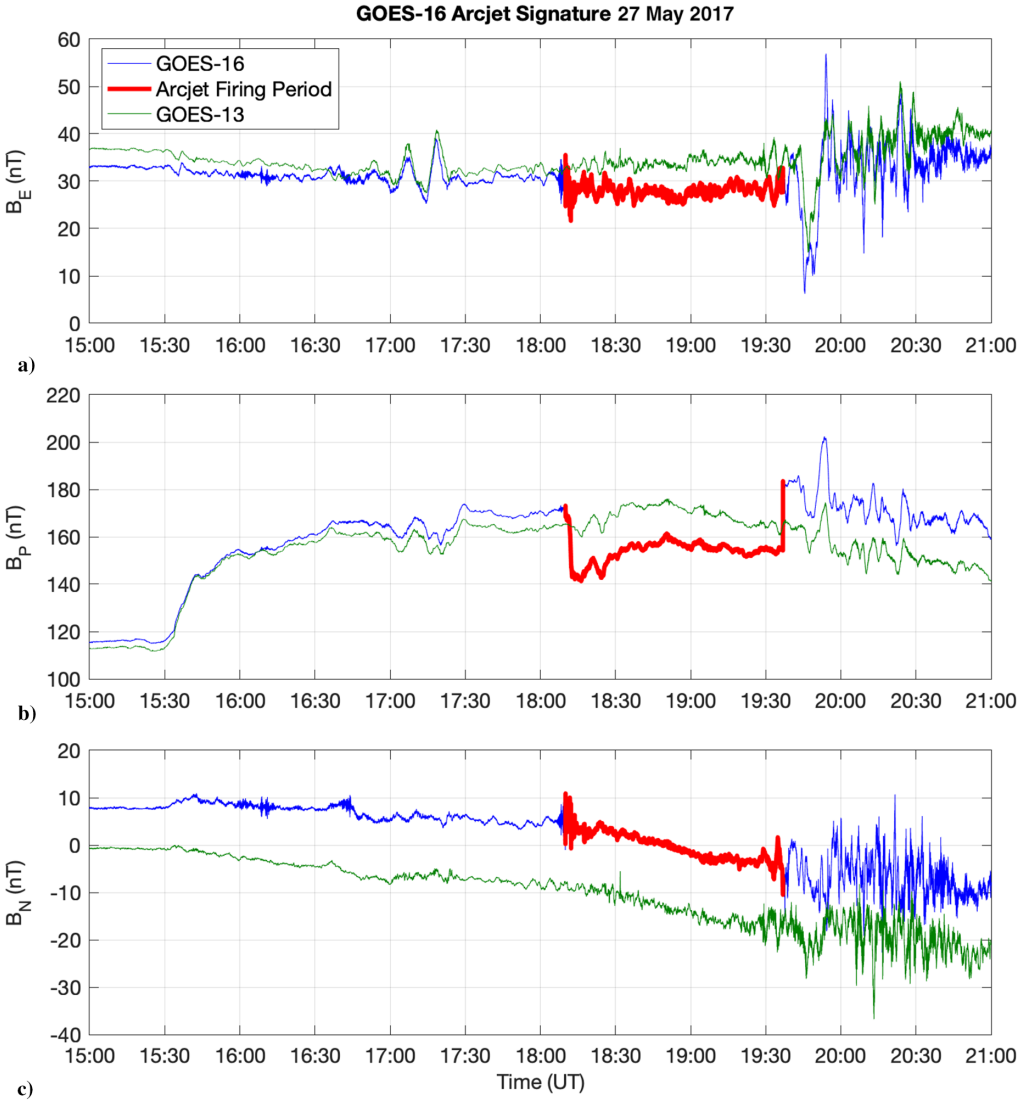

Fig. 2 Example of arcjet contamination (red region of curves) on the GOES-16 outboard magnetometer in Earth-poleward-normal coordinates.

thrusters. The two steps in Fig. 4 correspond to the current being turned off to each thruster one at a time. As opposed to the slow startup transients in Fig. 3, the turn-off transients are very rapid, allowing the arcjet effect to be more easily distinguished from geophysical variations.

The thrusters are fired in pairs, and so the difference between the "on" measurements and the "off" measurements represent the total effect of two arcjet thrusters. The effect of the first thruster to be turned off is estimated by the difference between the on and "mid-" measurements, and the effect of the second thruster is the difference between the mid- and off measurements. The off magnetic field at the outboard magnetometer is used to estimate the undisturbed ambient geomagnetic field. There are bias differences between the inboard and outboard magnetometers that are caused by known calibration issues on GOES-16, and the outboard magnetometer is considered to be more accurate [8]. Also, the arcjet operation affects the magnetometer electronics temperature, introducing a small bias that decays over 1–2 h after the burn.

IV. Arcjet Signature Dependence on the Ambient Magnetic Field

To determine a probable mechanism for the arcjet magnetic field contamination, the magnitude of the change in the magnetic field due to arcjet thruster firings was correlated with the ambient magnetic field strength. This is shown in Fig. 5, where the change in the measured field at the outboard magnetometer, which was derived by differencing the on and off measurements described in the previous section, is plotted against the undisturbed ambient magnetic field determined 1 s after the thrusters are turned off. The thrusters fire in pairs, using either thrusters 13/15 or 14/16 (see Fig. 1). The results in Fig. 5 show the combined effect of each thruster pair at both the inboard (closed circles) and outboard magnetometers (open circles) in the spacecraft-fixed ACRF coordinate system.

Figure 5 shows that the largest response is in the Y axis, which is aligned along the thrust vector (the thruster nozzle points in the $-Y$ direction), and that the change in the measured magnetic field scales linearly with the ambient magnetic field in the Y direction. This results in a reduction in the ambient magnetic field amplitude and is likely caused by a diamagnetic effect (see Sec. V) due to the dense thruster plume plasma. The Y axis is nominally approximately antialigned with the main component of the geomagnetic field, although the field direction can vary by up to ~45 deg. The correlation between the contamination and the ambient field strength along the Y axis is independent of the alignment of the ambient field and the thruster.

In the X and Z axes, there is no clear correlation between the arcjet signatures and the strength of the ambient magnetic field. However, the magnitudes of the X and Z components of the contamination are different between the inboard and outboard magnetometers. The arcjet effect is stronger by several nanotesla at the inboard magnetometer, indicating that the source of the magnetic contamination is localized near the spacecraft. Also, the trends are similar in the inboard and

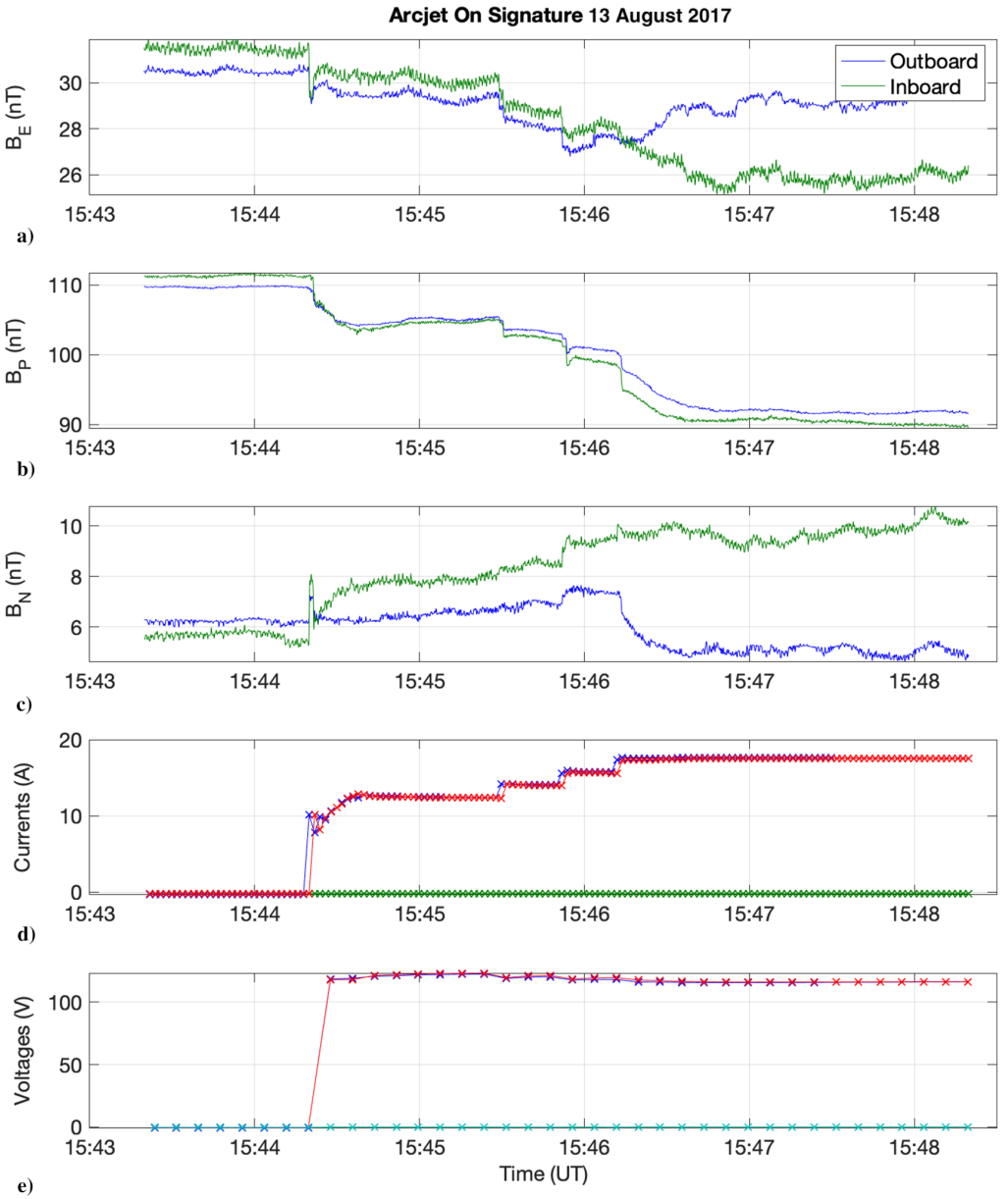

Fig. 3 Example startup arcjet transient on 13 August 2017: a–c) measured magnetic field at inboard and outboard magnetometers in EPN coordinates, d) thruster currents, and e) thruster voltages indicating start of arcjet firing.

outboard observations, but the arcjet effect is more variable at the inboard magnetometer.

In Fig. 6, the effect of individual thrusters is shown using the intermediate step responses (see Fig. 4) as the thrusters are sequentially turned off. The slope of the proportional response in the Y axis is similar for all four thrusters, and the offsets at each magnetometer are organized by thruster location. Thrusters 13 and 14 are located close together near the $-X$ side of the $-Y$ panel of the spacecraft, and thrusters 15 and 16 have the same relative spacing but are on the opposite side $(+X)$ of the $-Y$ panel, closer to the magnetometers. The magnetometer boom extends 30 deg from the $-Z$ axis deflected toward $+X$ and $-Y$ (see Fig. 1). Thrusters 13 and 14 create a $+X/-Z$ change in the magnetic field; and thrusters 15 and 16, which are on the opposite side of the spacecraft and closer to the magnetometer boom, cause a $-X/+Z$ deflection in the measurement. In addition to the diamagnetic proportional effect, there are also offsets in the Y axis that depend on the relative locations of thrusters and magnetometers.

V. Discussion of Physical Mechanisms

The results shown in Figs. 5 and 6 indicate that the arcjet contamination can be separated into a proportional reduction in the ambient magnetic field amplitude along the thrust axis and offsets that depend on the relative locations of the thrusters and the magnetometers. Hence, it is suggested that there are two separate physical mechanisms at play producing the total contamination: 1) a large-scale diamagnetic effect caused by the dense plasma in the thruster plume that is proportional to the ambient field strength, and 2) a local current source near the spacecraft caused by plasma pressure gradients in the thruster plume that does not depend on the ambient magnetic field. This section discusses the physics of these two mechanisms.

A. Proportional Response

The arcjets apply a current to the neutral hydrazine propellant that partially ionizes the thruster plume, creating a very dense plasma relative to the ambient environment that interacts with the ambient geomagnetic field. Although the arcjet plume is only ~1% ionized [10], the plasma density of the plume was measured to be $\sim 10^{12}$ m^{-3} in ground tests [11], which is several orders of magnitude larger than the typical ambient low-energy electron density at geostationary orbit. The linear responses in Figs. 5 and 6 along the Y axis suggest this interaction results in a diamagnetic effect where the plasma creates an opposing magnetic field to the background field due to the

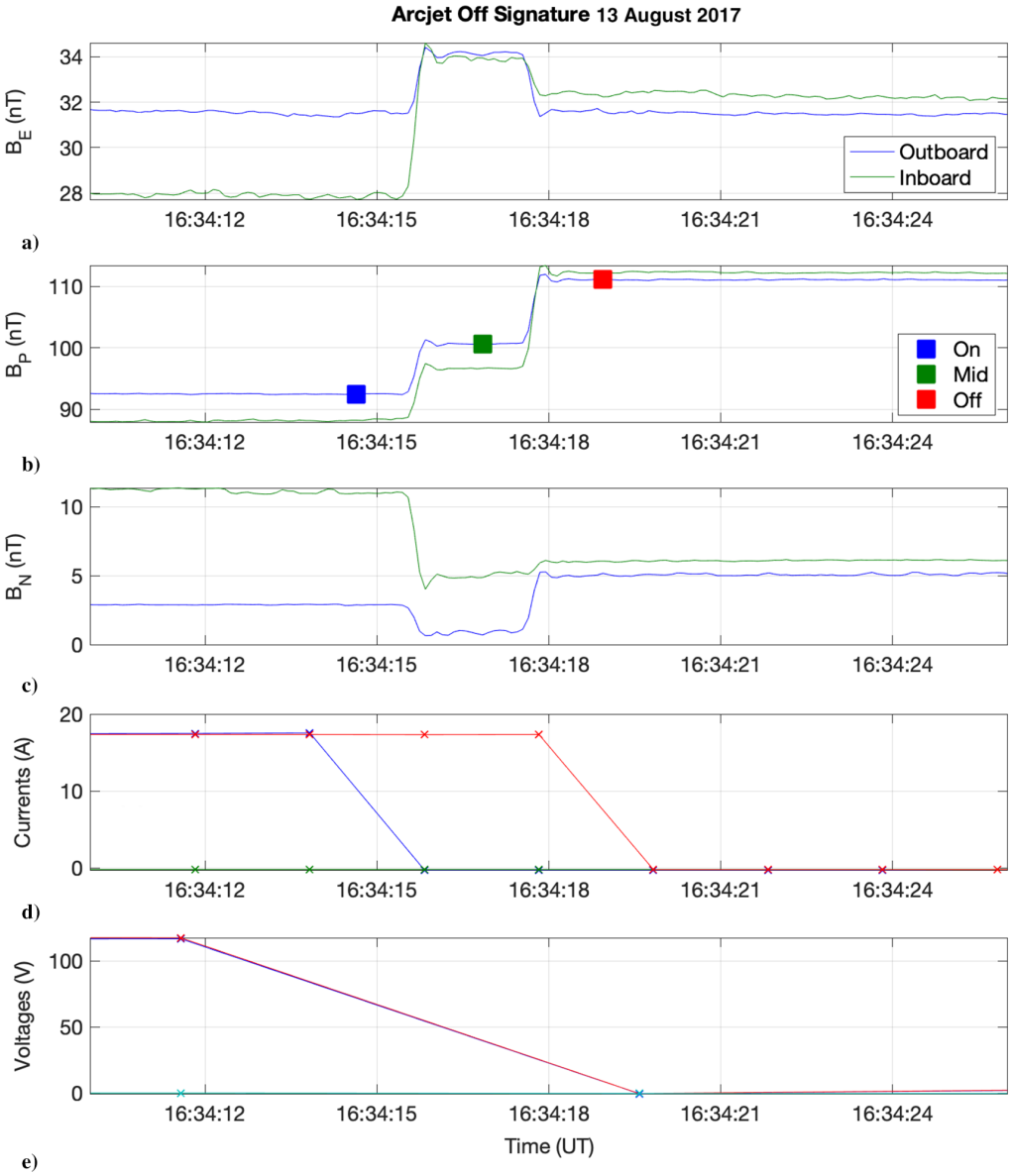

Fig. 4 Arcjet signature as the thrusters are turned off on 13 August 2017: a–c) measured magnetic field at inboard and outboard magnetometers in EPN coordinates, d) thruster currents, and e) thruster voltages.

gyromotion of the charged particles about the magnetic field. Here, the observed linear relationship between the change in the magnetic field from the arcjet thrusters and the strength of the ambient magnetic field is derived.

The diamagnetic effect can be described through a balance between the ambient pressure external to the plume and the pressure inside the thruster plume. Total pressure P, is given by

$$P = P_{\text{particle}} + P_{\text{magnetic}} \tag{1}$$

where $P_{\text{particle}} + P_{\text{magnetic}}$ are the plasma particle pressure and the magnetic pressure, respectively.

In the ambient environment at geostationary orbit, the magnetic pressure typically dominates the plasma pressure, and we can ignore the ambient plasma contribution to the total pressure. The ambient pressure outside of the thruster plume P_0, is written as

$$P_0 = \frac{B_0^2}{2\mu_0} \tag{2}$$

The total pressure inside the thruster plume P_1, is given by the sum of the particle pressure from the plume plasma P_{plume}, and the local magnetic pressure within the plume:

$$P_1 = P_{\text{plume}} + \frac{B_1^2}{2\mu_0} \tag{3}$$

In equilibrium, the pressure inside the thruster plume is equal to the ambient pressure outside of the plume. When the relatively dense plasma from the plume is injected into the ambient environment, the local magnetic field decreases to balance the total pressure inside the plume with the ambient pressure outside the plume. By writing B_1 as the sum of the ambient field B_0 and the change in the field ΔB, the change in the magnetic field can be expressed as a function of the ambient magnetic field. Setting the pressure inside the plume P_1, equal to the external ambient pressure P_0, gives

$$\frac{B_0^2}{2\mu_0} = P_{\text{plume}} + \frac{(B_0 + \Delta B)^2}{2\mu_0} \tag{4}$$

Expanding Eq. (4) results in

$$\frac{B_0^2}{2\mu_0} = P_{\text{plume}} + \frac{B_0^2 + 2B_0\Delta B + \Delta B^2}{2\mu_0} \tag{5}$$

Because ΔB is small relative to B_0, the higher-order term ΔB^2 can be ignored. Rearranging Eq. (5) produces the change in the magnetic

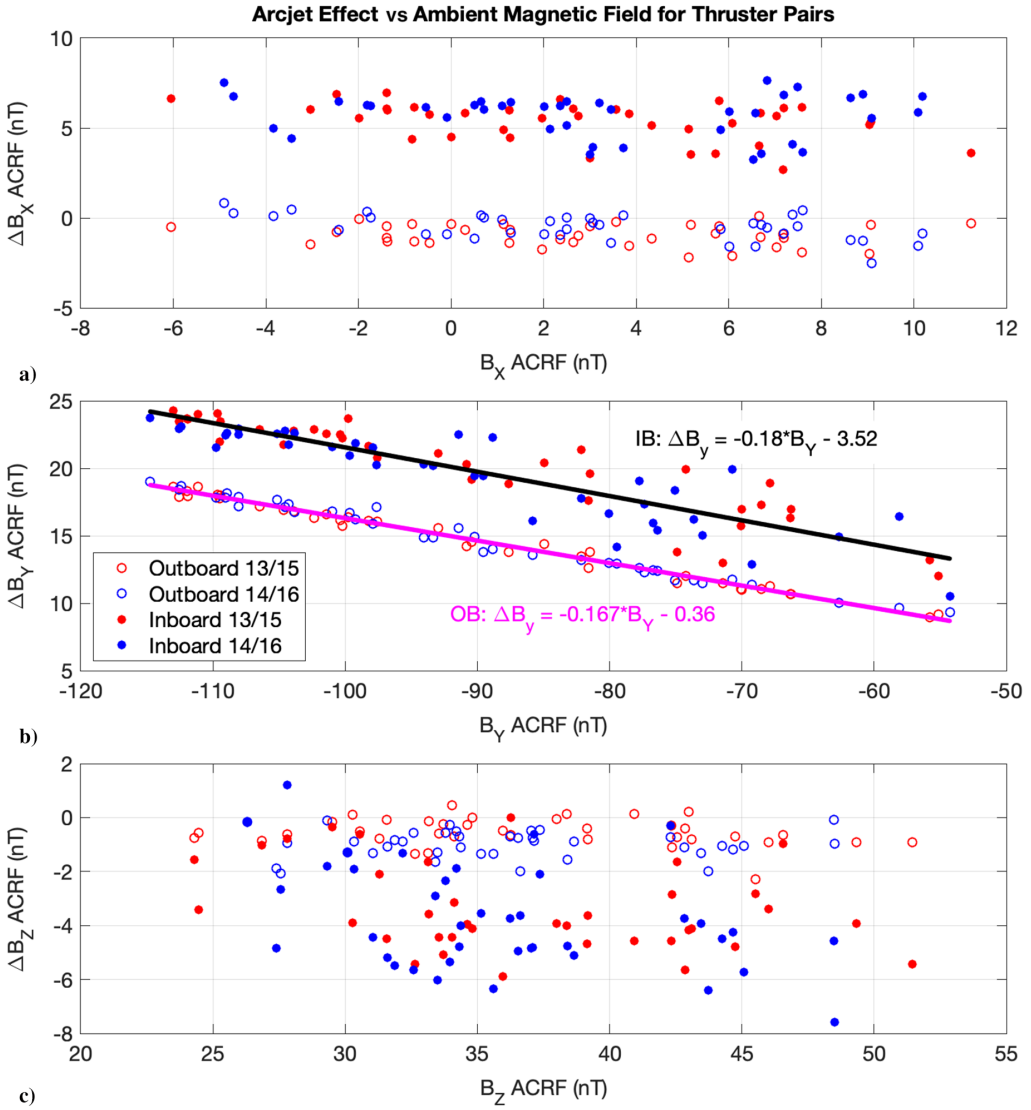

Fig. 5 Arcjet response ΔB as a function of ambient magnetic field for thruster pairs.

field due to the arcjets ΔB, as a function of plume plasma pressure P_{plume}:

$$\Delta B = -\frac{\mu_0 P_{\text{plume}}}{B_0} \tag{6}$$

Equation (6) predicts the change in the local magnetic field to be proportional to $(1/B_0)$ if the plasma pressure in the plume is constant across arcjet firings, but the data in Figs. 5 and 6 show that the change in B_y is proportional to B_0. We explain this discrepancy in the following:

It can be assumed that the expected mass flow rate of the thruster, percent ionization, and thruster plume plasma temperature remain constant across the different arcjet events. Once the plasma is ejected, the pressure of the plasma in the plume varies with the strength of the background magnetic field as $\sim B_0^2$. A simple way to understand this relationship is that the gyroradius of the particles in the plume is given by

$$r_{\text{gyro}} = \frac{m v_\perp}{q B_0} \tag{7}$$

where m is the plasma particle mass, $v_\perp$ is the magnitude of the particle velocity perpendicular to the magnetic field, q is the charge, and B_0 is the strength of the magnetic field. Therefore, the area of the plume plasma, which is proportional to r_{gyro}^2, varies by $(1/B_0^2)$, meaning that a stronger background magnetic field constricts the size of the plasma plume. With the same number of particles being ejected in each thruster event, the density, and therefore the pressure, vary as B_0^2:

$$P_{\text{plume}} = C B_0^2 \tag{8}$$

where C is a scaling constant. Substituting this relationship into Eq. (6) results in the observed proportionality between the change in the magnetic field and the background field:

$$\Delta B = -\frac{\mu_0 C B_0^2}{B_0} = -\mu_0 C B_0 \tag{9}$$

For a typical 100 nT ambient magnetic field at geostationary orbit, the plume plasma pressure required to reduce the background magnetic field by 20% ($\Delta B = -20$ nT) is estimated by rearranging Eq. (4):

$$P_{\text{plume}} = \frac{B_0^2}{2\mu_0} - \frac{(B_0 + \Delta B)^2}{2\mu_0} = 1.4 \times 10^{-9}\ \text{Pa} \tag{10}$$

This simplified derivation of the diamagnetic effect assumes an isotropic pressure within the plume. In this scenario, the diamagnetic effect would act along the ambient magnetic field direction.

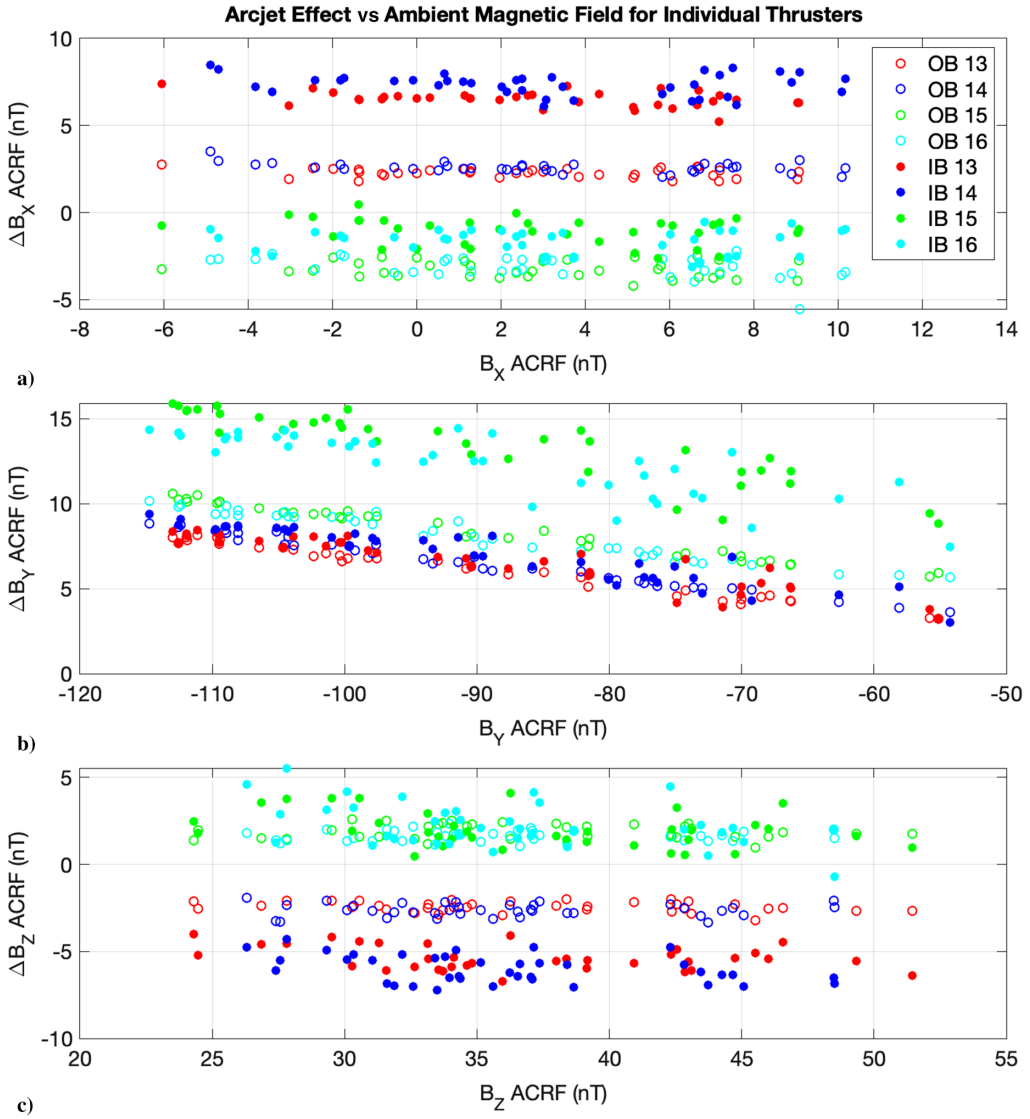

Fig. 6 Arcjet response ΔB as a function of ambient magnetic field for individual thrusters.

However, the diamagnetic relationship is only observed along the thrust axis (Figs. 5 and 6), and the effect does not depend on the angle between the ambient magnetic field and the thrust axis. In reality, the pressure from the arcjet is not isotropic, and it is strongest in the direction of the thruster nozzle: both due to the dynamic pressure from the bulk plasma flow and the increased density along the centerline of the plume. This pressure anisotropy causes the diamagnetic relationship to only appear in the thrust direction.

The plasma density within the plume can be estimated based on the particle pressure calculated in Eq. (10). The particle pressure in the plume has contributions from the random thermal velocity of the plasma (thermal pressure) and the plasma bulk flow velocity (dynamic pressure):

$$P_{\text{plume}} = nk(T_e + T_i) + \frac{1}{2}\rho V^2 \tag{11}$$

The mass density ρ, can be written in terms of the plasma number density n, and equivalent mass m_{eq}, which represents the average mass of the plasma particles:

$$\rho = nm_{\text{eq}} \tag{12}$$

$$P_{\text{plume}} = n\left(k(T_e + T_i) + \frac{1}{2}m_{\text{eq}}V^2\right) \tag{13}$$

Ground tests indicate that the plasma temperature is ~0.1 eV, and the flow velocity is ~7 km/s [11]. The ionized portion of the plume is dominated by Hydrons (H^+) and Nitrogen cations (N^+), but the ratios are not known precisely. Hydrazine is composed of Nitrogen Hydride (N_2H_4), and so a 2:1 ratio of H^+ to N^+ is assumed to provide a rough estimate of the plasma density based on the observed reduction in the magnetic field. The equivalent mass is

$$m_{\text{eq}} = 5.3\ \text{m}_{\text{proton}} = 8.85 \times 10^{-27}\ \text{kg} \tag{14}$$

Rearranging Eq. (13) and solving for density results in

$$n = \frac{P_{\text{plume}}}{k(T_e + T_i) + (1/2)m_{\text{eq}}V^2} = 5.8 \times 10^9\ \text{m}^{-3} \tag{15}$$

Likar et al. [11] created a model of the plasma density based on laboratory measurements given by

$$n = 9.2 \times 10^{12} z^{-2.19}\ \text{cm}^{-3} \tag{16}$$

where z is the distance from the thruster nozzle in centimeters. Equation (16) predicts a plasma density of 3.5×10^{12} m^{-3} at the outboard magnetometer, which is more than two orders of magnitude larger than the estimate based on the observed diamagnetic reduction in the magnetic field [Eq. (15)]. The plasma density from Eq. (16)

Table 1 Correlation between the change in *Y*-axis magnetic field during arcjet firings and the *Y* component of the ambient magnetic field

	Outboard MAG		Inboard MAG	
Thruster pair	dBy/By	Correlation coefficient	dBy/By	Correlation coefficient
13/15	−0.165	−0.994	−0.179	−0.915
14/16	−0.168	−0.991	−0.182	−0.888

equals the estimated density from magnetic field deviations at a distance of 159 m from the thruster.

The plasma rapidly expands in the space environment, so this result suggests that the diamagnetic effect is related to the average plasma density over a much larger spatial scale than the length of the boom, rather than the local plasma density near the magnetometers. For reference, the electron and proton gyroradii in a 100 nT field assuming at temperature of 0.1 eV are 10 m and 450 m, respectively. An N^+ ion has a 1.7 km gyroradius under the same conditions, so the size of the diamagnetic cavity could be on the order of hundreds of meters to kilometers. This analysis also shows that the ground-based density estimates of the plume plasma [11] are sufficient to produce the observed diamagnetic variations in the local magnetic field.

Table 1 shows the correlation between the arcjet response and the ambient field for both thruster pairs at each magnetometer. The values are calculated using the difference between the on and off measurements at the end of the arcjet burn (see Fig. 4). The proportional relationship is similar for each thruster pair, but the slope at the inboard magnetometer is ∼8% larger than the slope at the outboard magnetometer. The similar responses at the inboard and outboard magnetometers, which are located 6.3 and 8.5 m from the spacecraft, are an additional indication that the arcjets produce a diamagnetic cavity with a scale size that is much larger than the spacecraft and magnetometer boom.

B. Static Offsets

The diamagnetic response in the *Y* axis is the dominant effect on the magnetometer measurement, with total field variations of ∼10–20 nT that are proportional to the strength of the ambient magnetic field. In the *X* and *Z* axes, the offsets introduced by the arcjets are mostly independent of the ambient field; there are weak correlations in *X* and *Z*, but they are overwhelmed by the scatter in the data. In the *Y* axis, the linear fit to the data does not cross through the origin, indicating that the arcjets also create an offset in the *Y* axis. The offsets that are not proportional to the ambient field are referred to as static offsets, and they are assumed to be generated by a separate mechanism.

The static offsets for each thruster at the inboard and outboard magnetometers are summarized in Table 2. The *X* and *Z* values are determined by averaging the *X* and *Z* magnetic field deviations across all arcjet events, and the *Y* values are the intercepts from a linear fit between the change in the magnetic field and the ambient field, which removes the diamagnetic component of the response. At the outboard magnetometer, all four thrusters create an effect of similar magnitude (∼3.6–3.9 nT), but the directions are separated by ∼160 deg between the 13/14 and 15/16 thrusters. The thrusters fire in opposite pairs and the individual static offsets nearly cancel each other; so, the net static offset at the outboard magnetometer for each arcjet event is only ∼1.2 nT.

The static offsets are larger at the inboard magnetometer, and the net effects of the thruster pairs do not cancel as they do for the outboard magnetometer. Studying the combined effect of the thruster pairs can be misleading because there are likely two distinct magnetic sources (one for each thruster) that are superimposed during each arcjet event.

The original purpose of having inboard and outboard magnetometers was to subtract magnetic interference from the spacecraft using the gradiometric technique [12,13]. If the magnetometers are located at a sufficient distance from a magnetic source, the magnetic field magnitude is expected to decrease as $\sim 1/r^3$. Given the relative spacing of the inboard and outboard magnetometers on the boom, magnetic sources at the spacecraft are expected to be ∼2.4 times stronger at the inboard magnetometer than at the outboard magnetometer.

The differences between the arcjet responses at the outboard and inboard magnetometers for each event are plotted against the ambient magnetic field strength in Fig. 7. The lack of a clear relationship between the outboard–inboard difference and the ambient magnetic field in the *Y* direction is yet another indication that the scale size of the diamagnetic effect is much larger than the spacecraft and magnetometer boom; the diamagnetic behavior is essentially the same at the inboard and outboard locations. The static offsets, on the other hand, are organized by the thruster and magnetometer locations, indicating a separate localized current source. Table 3 summarizes the differences between the inboard and outboard magnetometers. The ratio of the inboard/outboard magnitudes is larger for the 13/14 thrusters than the 15/16 thrusters, and the direction of the disturbance is rotated by ∼20 deg and ∼50 deg between the magnetometers for the 13/14 and 15/16 thrusters, respectively.

One hypothesis for the static offset effect is a stray current loop at the spacecraft caused by the current that drives the arcjet thrusters closing through an unintended path on the spacecraft. This would alter the local magnetic field independently of the ambient magnetic

Table 2 Summary of static offsets related to arcjet thruster pairs and individual arcjet thrusters at the inboard and outboard magnetometers

Thruster	OB *X* offset, nT	OB *Y* offset, nT	OB *Z* offset, nT	OB Offset magnitude, nT	IB *X* offset, nT	IB *Y* offset, nT	IB *Z* offset, nT	IB Offset magnitude, nT
13/15	−0.974	−0.269	−0.542	1.15	5.7	3.97	−0.423	7.48
13	2.25	−1.32	−2.44	3.58	6.65	−0.315	−4.19	8.42
15	−3.23	1.05	1.9	3.89	−0.954	4.29	3.77	4.85
14/16	−0.515	−0.46	−0.991	1.21	5.83	3.08	1.39	7.51
14	2.58	−1.39	−2.63	3.93	7.44	−1.1	−4.06	9.56
16	−3.09	0.931	1.63	3.62	−1.61	4.18	5.44	5.02

Table 3 Summary of differences between static arcjet offsets at the inboard and outboard magnetometers

Thruster	OB-IB *X*, nT	OB-IB *Y*, nT	OB-IB *Z*, nT	IB/OB ratio	OB-IB angle, deg
13	−4.23	−1.01	2.92	2.35	21
14	−4.78	−0.287	3.38	2.43	15.4
15	−2.11	−3.23	−0.0792	1.25	51
16	−1.46	−3.25	−0.615	1.39	46.1

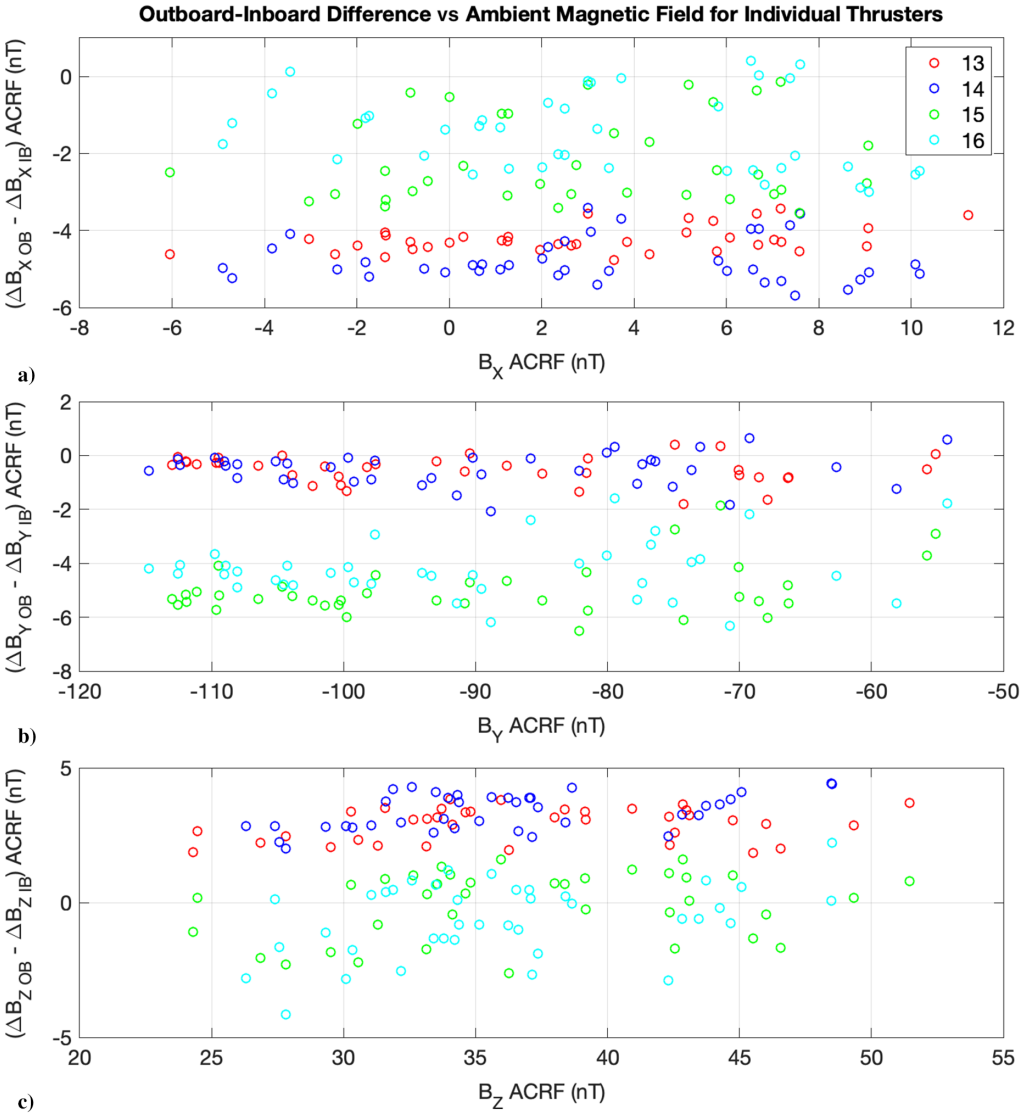

Fig. 7 Difference between the arcjet effect ΔB at the outboard and inboard magnetometers separated by thruster.

field strength. However, the scaling and rotation of the disturbance between the two magnetometers do not indicate a magnetic source at the spacecraft or near the thruster nozzles.

Alternatively, the static effect could be caused by localized pressure gradients within the thruster plume. The magneto-hydrodynamic force balance equation is

$$\nabla \cdot P = J \times B \tag{17}$$

The pressure gradients ∇P, are balanced by currents J, that, in turn, alter the magnetic field B, through

$$\nabla \times B = \mu_0 J \tag{18}$$

Near the thruster, the plasma plume dynamics are likely dominated by the thruster geometry and collisions with the dense neutral component of the plume rather than the relatively weak ambient geomagnetic field [14]. This would create consistent plasma geometry near the thrusters across arcjet events that is independent of the ambient magnetic field. At larger-scale sizes, the plume is more dispersed and gyromotion effects related to the ambient magnetic field become more important. This could explain a large-scale diamagnetic effect that is similar at the inboard and outboard magnetometers, as well as a smaller-scale localized pressure gradient effect that creates the observed static offsets.

VI. Conclusions

The GOES-16 magnetometer provides important operational space weather information that is used for forecasts and alerts by the NOAA's Space Weather Prediction Center. The GOES magnetometer data have also played an important role in the space physics scientific field, which develops the knowledge necessary to create operational products that meet the future needs of the user community. The arcjet thrusters on GOES-16 and the future GOES-R series cause a significant disturbance to the local magnetic field that periodically degrades the operational and scientific utility of the magnetometer data. By examining the rapid step response as the thrusters were turned off, a repeatable response in the magnetic field disturbance was revealed that is correlated with the ambient magnetic field. This repeatability will enable a correction algorithm that will remove much of contamination during arcjet events and allow the data to be used in operations. The correction algorithm is currently under development and will be applied to future publicly available GOES-R series magnetometer data.

There are two distinct magnetic signatures related to the arcjet thrusters: a ~20% proportional reduction in the ambient magnetic field along the thrust axis, and a smaller offset with components in all three axes that is independent of the ambient field. The proportional response is consistent with a diamagnetic effect due to the relatively dense plasma in the arcjet plume. Based on the similar proportional signatures at the inboard and outboard magnetometers, the diamagnetic effect likely occurs on a scale size that is much larger than the spacecraft.

The static offsets, which are fairly consistent regardless of the ambient magnetic field strength, vary in magnitude and direction depending on the relative positions of the thruster and magnetometer. These offsets are suggested to be driven by local plasma pressure gradients within the thruster plume. The physical mechanisms proposed in this study should be tested using detailed simulations of the spacecraft, arcjet thrusters, and the ambient plasma environment.

The arcjet contamination on the GOES-16 MAG was not predicted by preflight ground tests, and it may not be possible to reproduce the effect in a laboratory environment because of the difficulty in creating flightlike conditions on the ground [4]. Ground tests were performed on similar arcjet thrusters to the GOES arcjets to characterize the plume density, temperature, flow velocity, and ac electromagnetic effects [1,8]. These tests mainly focused on the arcjet impacts on communication systems, spacecraft charging, and solar array degradation. Bogorad et al. [1] measured the dc magnetic field near the arcjet and found no evidence of contamination, but the sensitivity of the test magnetometer was only 100 nT, whereas the observed effect on GOES-16 is ∼20 nT. The typical magnitude of the geomagnetic field at geostationary orbit is 100 nT. Conducting ground tests that can detect a 10–20 nT signal are challenging because of magnetic contamination in the laboratory and the need to cancel the Earth's magnetic field, which is ∼40,000 nT.

Ground tests and modeling should be validated with direct measurements of the thruster plasma in the specific orbital environment of interest in order to understand the interaction of electric thruster plumes with the spacecraft and scientific instruments. This study is effectively an active experiment that measured the magnetic response of arcjet thrusters using onboard scientific instruments. Future missions that use electric propulsion should be aware that these systems can impact sensitive scientific instruments and other spacecraft subsystems in ways that are not obvious through ground tests, and that these issues may only reveal themselves in the unique operational environment of a particular spacecraft.

Acknowledgments

Contributions from the National Oceanic and Atmospheric Administration's National Centers for Environmental Information by S. Califf and T. M. Loto'aniu were funded under GOES-R contract NA17OAR4320101. Work at NASA Goddard Space Flight Center was supported by the GOES-R Flight Project, with D. Early funded by contract NNG15CR65C and M. Grotenhuis funded by contract 80GSFC18C0120.

References

[1] Bogorad, A., Likar, J., Deeter, M., August, K., Doorley, G., and Herschitz, R., "Radiated Emissions and Magnetic Field Characterization of a 2-kW Electrothermal Propulsion System," *IEEE Transactions on Electromagnetic Compatibility*, Vol. 50, No. 3, 2008, pp. 466–475. https://doi.org/10.1109/TEMC.2008.927941

[2] Grebnev, I., Ivanov, G., Khodnenko, V., Morozov, A., Perkov, I., Pertsev, A., Romanovsky, J., Rylov, J., Shishkin, G., and Trifonov, J., "The Study of a Plasma Jet Injected by an On-Board Plasma Thruster," *Advances in Space Research*, Vol. 1, No. 2, 1981, pp. 153–158. https://doi.org/10.1016/0273-1177(81)90284-2

[3] Gabdullin, F., Korsun, G., and Tverdokhlebova, E., "The Plasma Plume Emitted Onboard the International Space Station Under the Effect of the Geomagnetic Field," *IEEE Transactions on Plasma Science*, Vol. 36, No. 5, 2008, pp. 2207–2213. https://doi.org/10.1109/TPS.2008.2004236

[4] Manzella, D., Jankovsky, R., Elliott, F., Mikellides, I., Jongeward, G., and Allen, D., "Hall Thruster Plume Measurements On-Board the Russian Express Satellites," *27th International Electric Propulsion Conference*, Electric Rocket Propulsion Soc. Paper 2001-044, Pasadena, CA, 2001.

[5] Huba, J. D., Bernhardt, P. A., Fedder, J. A., Lyon, J. G., and Mitchell, H. G., "Modelling the Plasma Dynamics of the CRRES G-9 and G-10 Barium Releases," *Advances in Space Research*, Vol. 13, No. 10, 1993, pp. 45–54. https://doi.org/10.1016/0273-1177(93)90049-H

[6] Tsyganenko, N. A., and Sitnov, M. I., "Modeling the Dynamics of the Inner Magnetosphere During Strong Geomagnetic Storms," *Journal of Geophysical Research*, Vol. 110, No. A3, 2005, Paper A03208. https://doi.org/10.1029/2004 JA010798

[7] Singer, H. J., Matheson, L., Grubb, R., Newman, A., and Bouwer, S. D., "Monitoring Space Weather with the GOES Magnetometers," *GOES-8 and Beyond: Proceedings of the SPIE*, Vol. 2812, edited by E. R. Washwell, International Soc. for Optical Engineering, Bellingham, WA, 1996, pp. 299–308. https://doi.org/10.1117/12.254077

[8] Loto'aniu, T. M., Redmon, R., Califf, S., Singer, H. J., Rowland, W., Macintyre, S., Chastain, C., Dence, R., Bailey, R., Shoemaker, E., et al., "The GOES-16 Spacecraft Science Magnetometer," *Space Science Reviews*, Vol. 215, No. 4, 2019, Paper 32. https://doi.org/10.1007/s11214-019-0600-3

[9] Gosling, J. T., McComas, D. J., Phillips, J. L., and Bame, S. J., "Geomagnetic Activity Associated with Earth Passage of Interplanetary Shock Disturbances and Coronal Mass Ejections," *Journal of Geophysical Research*, Vol. 96, No. A5, 1991, pp. 7831–7839. https://doi.org/10.1029/91 JA00316

[10] Carney, L. M., and Sankovic, J. M., "The Effects of Arcjet Thruster Operating Condition and Constrictor Geometry on the Plasma Plume," *25th Joint Propulsion Conference*, AIAA Paper 1989-2723, June 1989. https://doi.org/10.2514/6.1989-2723

[11] Likar, J., Bogorad, A., Malko, T., Goodzeit, N., Galofaro, J., and Mandell, M., "Interaction of Charged Spacecraft with Electric Propulsion Plume: On Orbit Data and Ground Test Results," *IEEE Transactions on Nuclear Science*, Vol. 53, No. 6, 2006, pp. 3602–3606. https://doi.org/10.1109/TNS.2006.885107

[12] Ness, N., Behannon, K., Lepping, R., and Schatten, K., "Use of Two Magnetometers for Magnetic Field Measurements on a Spacecraft," *Journal of Geophysical Research*, Vol. 76, No. 16, 1971, pp. 3564–3573. https://doi.org/10.1029/JA076i016p03564

[13] Acuna, M., "Space-Based Magnetometers," *Review of Scientific Instruments*, Vol. 73, No. 11, 2002, pp. 3717–3736. https://doi.org/10.1063/1.1510570

[14] Korsun, A. G., Tverdokhlebova, E. M., and Gabdullin, F. F., "Earth's Magnetic Field Effect Upon Plasma Plume Expansion," *25th International Electric Propulsion Conference*, Electric Rocket Propulsion Soc. Paper 1997-178, Cleveland, OH, Aug. 1997.

J. T. Cassibry
Associate Editor